

Sensitivity on Anomalous Neutral Triple Gauge Couplings via ZZ Production at FCC-hh

A. Yilmaz*

Department of Electrical and Electronics Engineering, Giresun University, 28200, Giresun, Turkey

A. Senol† and H. Denizli‡

Department of Physics, Bolu Abant Izzet Baysal University, 14280 Bolu, Turkey

I. Turk Cakir§

Department of Energy Systems Engineering, Giresun University, 28200 Giresun, Turkey

O. Cakir¶

Department of Physics, Ankara University, 06100 Ankara, Turkey

We study the sensitivity of anomalous neutral triple gauge couplings (aNTGC) via $pp \rightarrow ZZ$ production in the 4ℓ channel at 100 TeV centre of mass energy of future circular hadron collider, FCC-hh. The analysis including the realistic detector effects is performed in the mode where both Z bosons decay into same flavor, oppositely charged lepton pairs. The sensitivities to the charge-parity (CP)-conserving $C_{\tilde{B}W}/\Lambda^4$ and CP-violating C_{WW}/Λ^4 , C_{BW}/Λ^4 and C_{BB}/Λ^4 couplings obtained at 95% Confidence Level (C.L.) using the invariant mass distribution of 4ℓ system reconstructing the leading and sub-leading Z boson candidates are $[-0.117, +0.117]$, $[-0.293, +0.292]$, $[-0.380, +0.379]$, and $[-0.138, +0.138]$ in the unit of TeV^{-4} , respectively.

I. INTRODUCTION

The studies on the diboson production at colliders play an important role in testing the non-Abelian $SU(2)_L \times U(1)_Y$ gauge group of the electroweak sector in the Standard Model (SM) and searching for new phenomena at the TeV-energy scale [1]. Since there is no triple gauge couplings between the photon and Z boson ($Z\gamma\gamma$ and $Z\gamma Z$) except WWZ and $WW\gamma$ in the SM, pairs of Z bosons cannot be created at a single vertex in the SM. Therefore any deviations from SM predictions on neutral triple gauge couplings (including $ZZ\gamma$, $Z\gamma\gamma$ and ZZZ vertices) can give an indication about new physics beyond the SM. The new physics effects at high energy can be parametrized in the Effective Field Theory (EFT) approach. This theory is general enough to point the most probable places to observe these effects since it is renormalizable, includes the gauge symmetries of the standard model and can be used at both tree level and loop level. There is no concern on violating of the unitary of anomalous couplings in scattering processes at higher energies according to this theory. Anomalous NTG vertices can be added in an effective Lagrangian using EFT approach and parametrized by CP-conserving and CP-violating couplings, while no SM NTGC is present at tree-level [2].

The production of ZZ dibosons in the 4ℓ final state

have been studied by various collaborations such as the Large Electron-Positron (LEP) [3–8] where the first bounds on anomalous neutral triple gauge couplings (aNTGCs) using e^+e^- collider was obtained, the Collider Detector at Fermilab (CDF) [9, 10] and $D\bar{O}$ [11, 12] also searched the limits of aNTGC at Tevatron pp collider. Recently, ATLAS [13, 14] and CMS [15, 16] collaborations published the improved limits of aNTGCs thanks to the center of mass energy of LHC in the range of 13 TeV at the LHC. This high center of mass energy leads to enhance the cross-section which would widen the range of triple gauge coupling studies. There are also some phenomenological studies for probing the sensitivities of aNTGCs at hadron colliders in the EFT framework [17–21].

The dimension-eight (dim-8) effective Lagrangian for nTGC in the scope of EFT assuming the local $U(1)_{EM}$ and Lorentz symmetry can be written as [22]

$$\mathcal{L}^{nTGC} = \mathcal{L}_{SM} + \sum_i \frac{C_i}{\Lambda^4} (\mathcal{O}_i + \mathcal{O}_i^\dagger) \quad (1)$$

where i is the index of equations running over the operators given as

$$\mathcal{O}_{\tilde{B}W} = iH^\dagger \tilde{B}_{\mu\nu} W^{\nu\rho} \{D_\rho, D^\nu\} H, \quad (2)$$

$$\mathcal{O}_{BW} = iH^\dagger B_{\mu\nu} W^{\nu\rho} \{D_\rho, D^\nu\} H, \quad (3)$$

$$\mathcal{O}_{WW} = iH^\dagger W_{\mu\nu} W^{\nu\rho} \{D_\rho, D^\nu\} H, \quad (4)$$

$$\mathcal{O}_{BB} = iH^\dagger B_{\mu\nu} B^{\nu\rho} \{D_\rho, D^\nu\} H. \quad (5)$$

where $\tilde{B}_{\nu\mu}$ is dual B strength tensor. We used the

* aliylmaz@giresun.edu.tr

† senol.a@ibu.edu.tr

‡ denizli.h@ibu.edu.tr

§ ilkay.turk.cakir@cern.ch

¶ ocakir@science.ankara.edu.tr

convention given below in the definitions of the operators

$$B_{\mu\nu} = (\partial_\mu B_\nu - \partial_\nu B_\mu) \quad (6)$$

$$W_{\mu\nu} = \sigma^I (\partial_\mu W_\nu^I - \partial_\nu W_\mu^I + g\epsilon_{IJK} W_\mu^J W_\nu^K) \quad (7)$$

with $\langle \sigma^I \sigma^J \rangle = \partial^I \partial^J$ and

$$D_\mu \equiv \partial_\mu - ig_w W_\mu^i \sigma^i - i\frac{g'}{2} B_\mu Y \quad (8)$$

The coefficients of these four dimension-eight operators describing aNTGC are CP-conserving $C_{\tilde{B}W}/\Lambda^4$ and CP-violating C_{WW}/Λ^4 , C_{BW}/Λ^4 and C_{BB}/Λ^4 couplings.

The current limits on $C_{\tilde{B}W}/\Lambda^4$, C_{WW}/Λ^4 , C_{BW}/Λ^4 and C_{BB}/Λ^4 couplings of dim-8 operators converted from the couplings of dim-6 operators for the process $pp \rightarrow ZZ \rightarrow \ell^+ \ell^- \ell'^+ \ell'^-$ [14] where $\ell = e$ or μ and $Z\gamma \rightarrow \nu\bar{\nu}\gamma$ [23] at the center of mass energy $\sqrt{s} = 13$ TeV and integrated luminosity $L_{int} = 36.1 \text{ fb}^{-1}$ from the LHC are given in Table I. In this table, all couplings other than the one under study are set to zero.

TABLE I. Observed one dimensional 95% C.L. limits on $C_{\tilde{B}W}/\Lambda^4$, C_{WW}/Λ^4 , C_{BW}/Λ^4 and C_{BB}/Λ^4 EFT parameters from LHC.

Couplings (TeV^{-4})	Limit 95% C.L.	
	$ZZ \rightarrow 4\ell$ [14]	$Z\gamma \rightarrow \nu\bar{\nu}\gamma$ [23]
$C_{\tilde{B}W}/\Lambda^4$	-5.9, +5.9	-1.1, +1.1
C_{WW}/Λ^4	-3.0, +3.0	-2.3, +2.3
C_{BW}/Λ^4	-3.3, +3.3	-0.65, +0.64
C_{BB}/Λ^4	-2.7, +2.8	-0.24, +0.24

The future circular collider project, FCC [24], proposed to have three collider options (FCC-ee, FCC-eh and FCC-hh) working at different center of mass energies. The hadron collider option of FCC (FCC-hh) is planned to reach an integrated luminosity of 20-30 ab^{-1} at 100 TeV center mass energy. FCC-hh, comparing to LHC, has the energy scale by a factor about 7 depending on the process [25].

Exploring the new physics effects in the production of diboson is a challenging task. In the literature ZZ diboson production has been examined in 2 decay channels such as “ $2\ell 2\nu$ ” and “ 4ℓ ” channel [2]. In the first channel $ZZ \rightarrow 2\ell 2\nu$, one of the Z decays into a neutrino while the other one decaying into a same flavor, oppositely-charged two leptons which leads to increase in the missing transfer energy in the final state. Therefore this channel exposes to a larger background contribution and it is not kinematically reconstructable completely. In the second decay channel $ZZ \rightarrow 4\ell$, not only the first Z boson, but also the other Z boson decays into a same-flavor, oppositely charged two leptons. This process gives rise to include a very low background and kinematically reconstructable in the final state. On the other hand, one needs to take into account the process has small branching fractions results with a low statistics in the final state.

This paper will be organized as follows: In section II we will discuss the simulation environment of ZZ diboson production for signal and background at FCC-hh collider. Event selection procedures of our phenomenological study in the 4ℓ final state will be given in section III. In section IV, we will give the collected results for 4ℓ final state analysis. Conclusions on the sensitivities of each couplings will be summarized in section V.

II. GENERATION OF SIGNAL AND BACKGROUND EVENTS

To obtain the bounds on aNTGC parameters of ZZ diboson production in the framework of the EFT at the FCC-hh. We generated signal and background events for the $pp \rightarrow ZZ$ process by importing the signal aTGC implemented through UFO model file into MadGraph5_aMC@NLO v2.6.4 [26]. The PYTHIA v8.2 [27] package is used for parton showering and hadronization. LHAPDF v6.1.6 [28] library and its NNPDF v2.3 [29] set is used as the default set of parton distribution functions (PDFs) for all simulated MC samples. 3×10^6 events of the signal and the background were generated for each dim-8 couplings. The detector response is simulated using a detailed description of the FCC-hh detector card implemented in the Delphes v3.4.1 [30]. All events are analyzed by using the ExRootAnalysis [31] package with ROOT v6.16 [32]. The kinematical distributions are normalized to the number of expected events which is defined to be the cross section of each processes including the branchings times integrated luminosity of $\mathcal{L}_{int} = 10 \text{ ab}^{-1}$.

Feynman diagrams that contribute to the signal and its main-background processes are shown in Fig. 1(a) and Fig. 1(b), respectively. The red dot represents the aNTGC vertex in the production of ZZ .

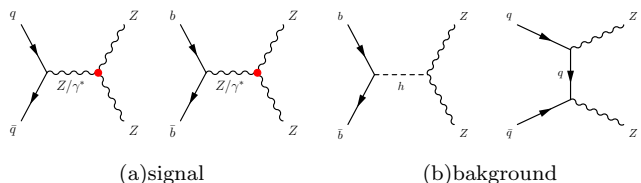


FIG. 1. Feynmann diagrams of ZZ production (a) for signal including an aNTGC vertex depicted by a red dot, (b) for the SM background.

The cross section is calculated with a set of generator level cuts; a lepton is declared to be isolated if the p_T -sum of all particles within the isolation cone size $R_{iso} = 0.3$, minimum $p_T = 10 \text{ GeV}$ and $|\eta| < 2.5$ for the charged leptons. In the calculations, default mass of the Z boson is used as 91.187 GeV.

The cross sections of the ZZ process as a function of mentioned four dim-8 couplings are shown in Fig. 2. In this figure, only one coupling at a time is varied from its

SM value and plotted as a function of couplings in the range of limits reported by CMS Collaboration [16]. One can clearly see the deviation from the SM.

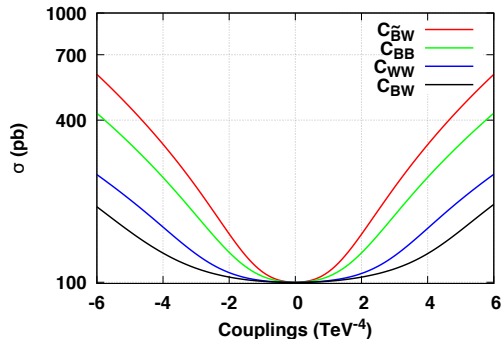


FIG. 2. Cross sections for the process with aNTGCs including CP-conserving and CP-violating terms in the Lagrangian.

III. EVENT SELECTION

We consider 4ℓ final state in our analysis based on Ref. [16] including three possible options; $e^+e^-e^+e^-$, $\mu^+\mu^-\mu^+\mu^-$, and $e^+e^-\mu^+\mu^-$. The preselection for this analysis require the presence of a pair of leptons of the same or different flavors [33]. All permutations of leptons giving a pair of Z/γ^* candidates are considered within each event. The pairing ambiguity is resolved by ordering the pair of dilepton candidates based on the differences between the reconstructed invariant mass of dilepton candidate ($m_{\ell+\ell^-}$) and nominal Z boson mass m_Z . Therefore, the dilepton candidate with an invariant mass closest to the nominal Z boson mass [34], is denoted *leading Z* while the second closest is defined as *subleading Z*.

In order to see the region where the signal can be enhanced we plotted the transverse momentum of leptons ($p_T^{\ell^1}, p_T^{\ell^2}$) versus the reconstructed invariant mass of the *leading* and *subleading Z* as shown in Fig. 3, Fig. 4 and Fig. 5 for $4e$, 4μ and $2e2\mu$ channels, respectively. $p_T^{\ell^1}$ is labelled as the highest- p_T lepton in both *leading* and *subleading Z*. The cut for highest $p_T^{\ell^1}$ lepton is greater than 20 GeV, and for the subleading lepton is $p_T^{\ell^2} > 12$ GeV (10 GeV) in the *leading Z*, while the remaining leptons in the *subleading Z* must have $p_T^{\ell^1, \ell^2} > 5$ GeV for electrons (muons).

The pseudo-rapidity cuts of all leptons are applied as $|\eta^\ell| < 2.5$. The distance $\Delta R(\ell^1, \ell^2)$ between leptons in η - ϕ plane is evaluated by the function

$$\Delta R(\ell^1, \ell^2) = \sqrt{(\eta^{\ell^1} - \eta^{\ell^2})^2 + (\phi^{\ell^1} - \phi^{\ell^2})^2} \quad (9)$$

and plotted in Fig. 6. This figure shows ΔR distributions between two leptons of *leading* and *subleading Z* in the first and second column. Each row corresponds

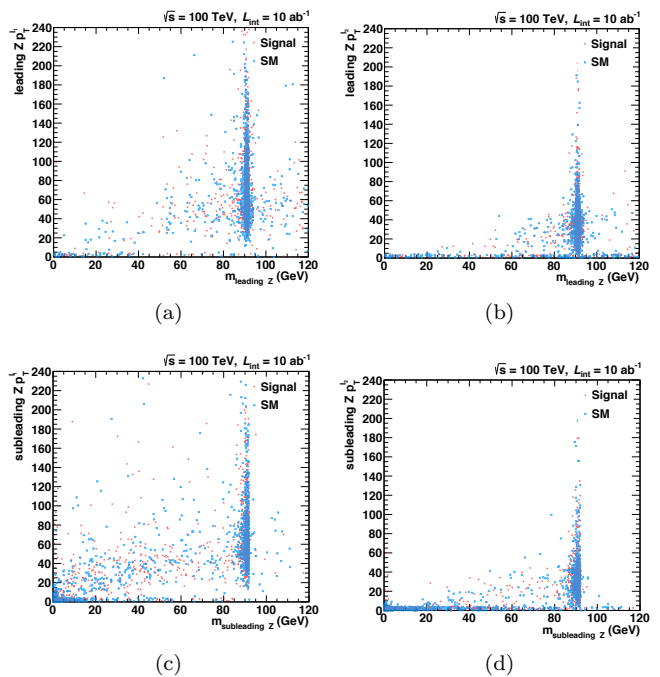


FIG. 3. Transverse momentum distributions of (a) leading lepton (b) subleading lepton of the *leading Z* boson vs its invariant mass and transverse momentum distributions of (c) leading lepton (d) subleading lepton of the *subleading Z* boson vs its invariant mass in the $4e$ channel.

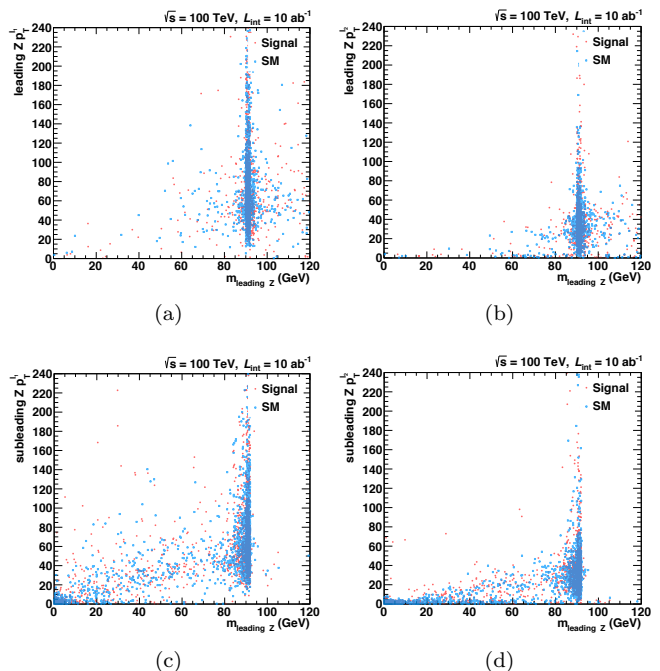


FIG. 4. Transverse momentum distributions of (a) leading lepton (b) subleading lepton of the *leading Z* boson vs its invariant mass and transverse momentum distributions of (c) leading lepton (d) subleading lepton of the *subleading Z* boson vs its invariant mass in the 4μ channel.

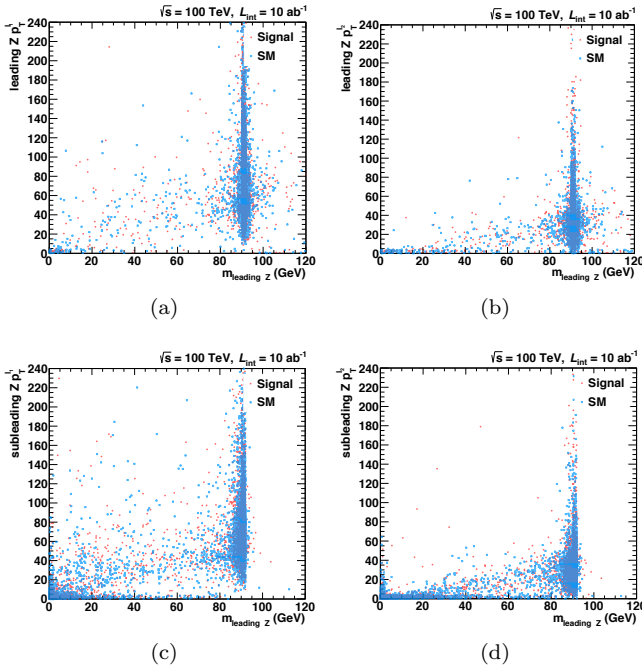


FIG. 5. Transverse momentum distributions of (a) leading lepton (b) subleading lepton of the *leading* Z boson vs its invariant mass and transverse momentum distributions of (c) leading lepton (d) subleading lepton of the *subleading* Z boson vs its invariant mass in the $2e2\mu$ channel.

to different decay channel aligned for $4e$, 4μ and $2e2\mu$, respectively. In order to meet the detector requirement, we applied a cut for all leptons are separated from each others by imposing $\Delta R(\ell^1, \ell^2) > 0.02$.

The $pp \rightarrow ZZ$ sensitivity is estimated by using events where a further cut is applied for both invariant mass of *leading* Z and *subleading* Z bosons must be within the range $80 < m_{\text{leading } Z} < 100$ GeV and $60 < m_{\text{subleading } Z} < 110$ GeV, respectively. This ranges were chosen to keep most of the decays in the resonance while removing mostly other processes with 4ℓ final states. Decays of the Z bosons to τ leptons with subsequent decays to electrons and muons are heavily suppressed by requirements on lepton p_T . The cut flow steps in the analysis for selecting the events are summarized in Table II.

After applying the kinematical cuts discussed above, the reconstructed invariant mass of the *leading* Z boson candidates, and a scatter plot showing the correlation between *subleading* Z boson versus *leading* Z boson in simulated events, are shown in Fig. 7.

IV. RESULTS

To obtain 95% C.L. limits on the couplings, we apply χ^2 criterion without and with a systematic error. The χ^2 function is defined as follows

$$\chi^2 = \sum_i^{n_{\text{bins}}} \left(\frac{N_i^{NP} - N_i^B}{N_i^B \Delta_i} \right)^2 \quad (10)$$

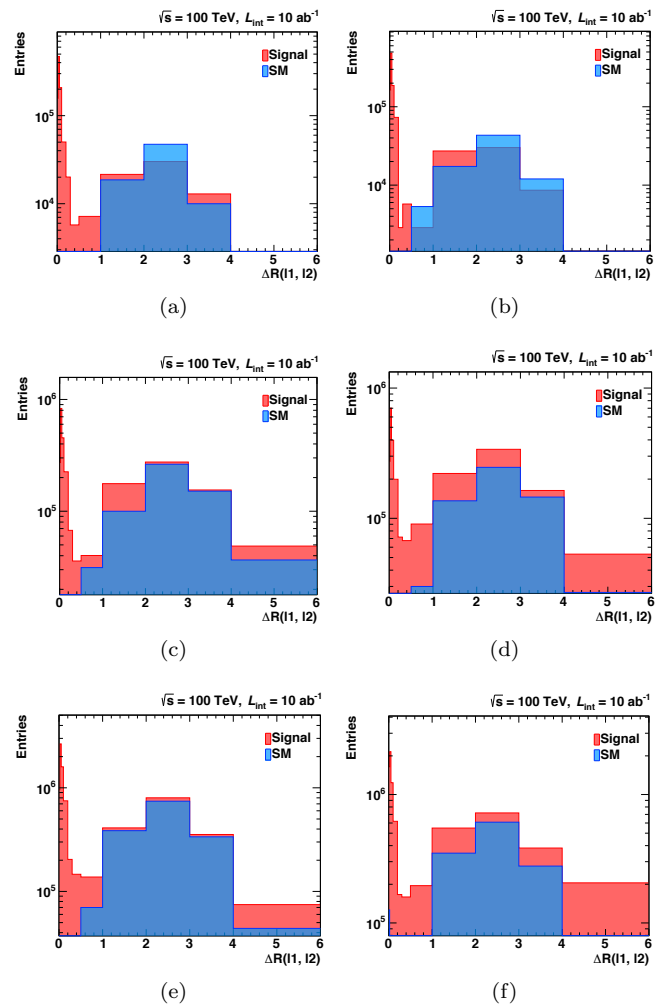


FIG. 6. ΔR distributions between leptons of candidate Z boson pairs in the $4e$ (a, b), 4μ (c, d) and $2e2\mu$ (e, f) channels. Fig. (a), (c) and (e) for *leading* Z and Fig. (b), (d) and (f) for *subleading* Z bosons.

TABLE II. Preselection and a set of cuts for the analysis of signal and background events.

Cuts	Definition
Cut-0	Preselection: $N_{\ell(e,\mu)} \geq 4$ and two same-flavor opposite-charge lepton pairs
Cut-1	Dileptons minimizing $ m_{\ell\ell}^a - m_Z + m_{\ell\ell}^b - m_Z $ are taken as Z boson pair candidates
Cut-2	Transverse momentum: $p_T^{\ell^1} > 20$ GeV, $p_T^{\ell^2} > 12$ GeV (10 GeV) for $e(\mu)$ and $p_T^{\ell^{3,4}} > 5$ GeV
Cut-3	Pseudo-rapidity: $ \eta^\ell < 2.5$
Cut-4	$\Delta R > 0.02$ between all leptons
Cut-5	Invariant mass: $80 < M_{\text{inv}}^{\text{rec}}(\text{leading } Z) < 100$ GeV and $60 < M_{\text{inv}}^{\text{rec}}(\text{subleading } Z) < 110$ GeV

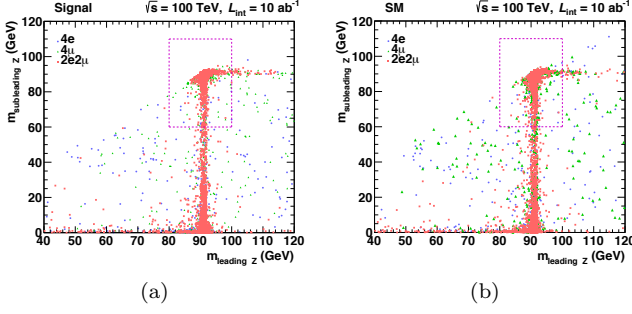


FIG. 7. Invariant mass distributions of *subleading* Z boson versus *leading* Z boson for signal (left) and main background (right) with an individual markers for each $4e$, 4μ and $2e2\mu$ channels.

TABLE III. The number of events yielded for main background and signal (where all couplings equal to zero, except $C_{\bar{B}W} = 5$) of four-lepton events in the mass region $80 < m_{4\ell} < 100$ GeV shown for each final state and combined at FCC-hh with $L_{\text{int}} = 10 \text{ ab}^{-1}$.

Channel	Signal	Background	Total
$4e$	16308	13991	30299
4μ	32477	26850	59327
$2e2\mu$	76404	71755	148159

where N_i^{NP} is the total number of events in the existence of effective couplings, N_i^B is total number of events of the corresponding SM backgrounds in i th bin of the invariant mass of the quartet-leptons distribution, $\Delta_i = \sqrt{\delta_{\text{sys}}^2 + 1/N_i^B}$ is the combined systematic (δ_{sys}) and statistical errors in each bin.

The existence of aTGCs will lead to enhance the yield of events at quadruplet-lepton masses. The distribution of the quadruplet-lepton reconstructed mass of events with both leading and subleading Z bosons in the mass range 60-120 GeV for the unified $4e$, 4μ , and $2e2\mu$ channels are depicted in Fig. 9. The limits on probable contributions from aNTGCs are extracted by using this distributions.

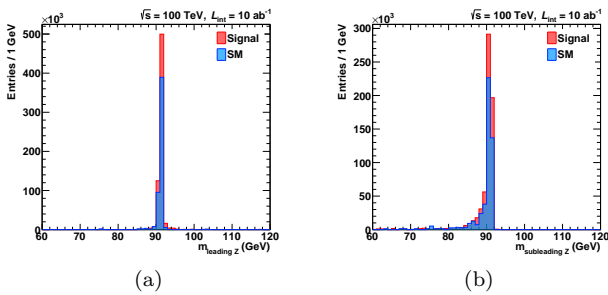


FIG. 8. Distributions of the reconstructed dilepton candidate mass for four-lepton events selected with both (a) leading and (b) subleading Z bosons on-shell.

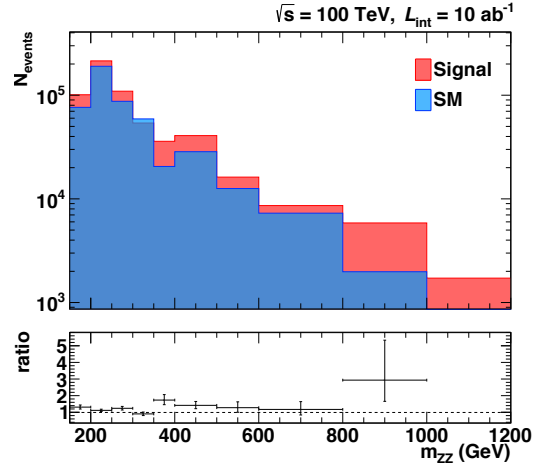


FIG. 9. Distributions of the reconstructed four-lepton invariant mass m_{ZZ} . In the m_{ZZ} distribution, bin contents are normalized to the bin widths. The lower plot shows the ratio of signal and background in each bin.

For the analysis of ZZ production with *quartet* – *leptons* in the final state, the number of signal events and one-parameter χ^2 results for each couplings varied with integrated luminosity from 1 ab^{-1} to 30 ab^{-1} . In the analysis, only one coupling at a time is varied from its SM value. The results from χ^2 analysis of the couplings describing aTGC interactions of neutral gauge bosons. The coefficients of the operators denoted as $C_{\bar{B}W}/\Lambda^4$, C_{WW}/Λ^4 , C_{BW}/Λ^4 and C_{BB}/Λ^4 are given in Fig. 10.

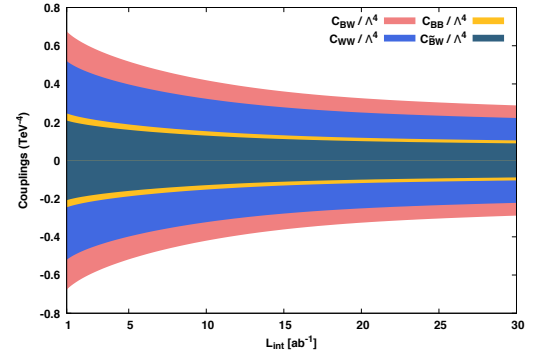


FIG. 10. Estimated sensitivity at 95% C.L. as a function of integrated luminosity where there is only one coupling varied at a time from its SM value.

We present the results of one-dimensional 95% C.L. confidence intervals at $L_{\text{int}} = 10 \text{ ab}^{-1}$ under the assumption that any excess in signal over background due exclusively to $C_{\bar{B}W}/\Lambda^4$, C_{WW}/Λ^4 , C_{BW}/Λ^4 or C_{BB}/Λ^4 are given in Table IV. We also include the effects of systematic errors on the limits. The obtained limits without systematic errors are one order better than the current limits on these couplings of *dim-8* operators converted from the couplings of *dim-6* operators for the process $pp \rightarrow ZZ \rightarrow \ell^+ \ell^- \ell'^+ \ell'^-$ [14] at the center of mass energy $\sqrt{s} = 13 \text{ TeV}$ and integrated luminosity $L_{\text{int}} = 36.1$

fb^{-1} from the LHC.

TABLE IV. Estimated one dimensional 95% C.L. limits on aNTG couplings with and without a systematic error at $L_{int} = 10 \text{ ab}^{-1}$. For each single anomalous coupling, all parameters other than the one under study are set to zero.

Couplings (TeV^{-4})	Limits at 95% C.L.			
	$\delta_{sys} = 0\%$	$\delta_{sys} = 1\%$	$\delta_{sys} = 3\%$	$\delta_{sys} = 5\%$
$C_{\bar{B}W}/\Lambda^4$	[-0.117, +0.117]	[-0.315, +0.315]	[-0.544, +0.544]	[-0.702, +0.702]
C_{WW}/Λ^4	[-0.293, +0.292]	[-0.805, +0.805]	[-1.388, +1.388]	[-1.792, +1.792]
C_{BW}/Λ^4	[-0.380, +0.379]	[-1.036, +1.036]	[-1.788, +1.788]	[-2.307, +2.307]
C_{BB}/Λ^4	[-0.138, +0.138]	[-0.373, +0.373]	[-0.644, +0.844]	[-0.831, +0.831]

V. CONCLUSION AND DISCUSSION

In this paper we present a phenomenological cut based study for probing the limits on the CP-conserving $C_{\bar{B}W}/\Lambda^4$ and CP-violating C_{WW}/Λ^4 , C_{BW}/Λ^4 and C_{BB}/Λ^4 dim-8 aNTG couplings via $ZZ \rightarrow 4\ell$ (where $\ell = e$ or μ) production at the FCC-hh.

The obtained limits of dim-8 aNTG couplings at 95% C.L. for $C_{\bar{B}W}/\Lambda^4$, C_{WW}/Λ^4 , C_{BW}/Λ^4 and C_{BB}/Λ^4 with

an $\mathcal{L}_{int} = 10 \text{ ab}^{-1}$ are one order better than those available prior to this study without systematic error. When we compare these results with the latest search for $\nu\bar{\nu}\gamma$ production [23] from the LHC, we have better results on $C_{\bar{B}W}/\Lambda^4$, C_{WW}/Λ^4 couplings and improved results on C_{BW}/Λ^4 and C_{BB}/Λ^4 couplings.

Even with 5% systematic errors, the obtained bounds for FCC-hh are better than the LHC results on all couplings studied in this paper. The limits of aNTG couplings would benefit from high luminosity and the high energy when the systematic uncertainties are well reduced below 5%.

VI. ACKNOWLEDGEMENT

This work was partially supported by Turkish Atomic Energy Authority (TAEK) under the project grant no. 2018TAEK(CERN)A5.H6.F2-20.

REFERENCES

- [1] M. S. Neubauer, *Annual Review of Nuclear and Particle Science* **61**, 223 (2011).
- [2] D. R. Green, P. Meade, and M.-A. Pleier, *Rev. Mod. Phys.* **89**, 035008 (2017), arXiv:1610.07572 [hep-ex].
- [3] R. Barate *et al.* (ALEPH), *Phys. Lett.* **B469**, 287 (1999), arXiv:hep-ex/9911003 [hep-ex].
- [4] M. Acciarri *et al.* (L3), *Phys. Lett.* **B465**, 363 (1999), arXiv:hep-ex/9909043 [hep-ex].
- [5] J. Abdallah *et al.* (DELPHI), *Eur. Phys. J.* **C30**, 447 (2003), arXiv:hep-ex/0307050 [hep-ex].
- [6] G. Abbiendi *et al.* (OPAL), *Eur. Phys. J.* **C32**, 303 (2003), arXiv:hep-ex/0310013 [hep-ex].
- [7] J. Alcaraz *et al.* (ALEPH, DELPHI, L3, OPAL, LEP Electroweak Working Group), (2006), arXiv:hep-ex/0612034 [hep-ex].
- [8] S. Schael *et al.* (ALEPH, DELPHI, L3, OPAL, LEP Electroweak), *Phys. Rept.* **532**, 119 (2013), arXiv:1302.3415 [hep-ex].
- [9] T. Aaltonen *et al.* (CDF), *Phys. Rev. Lett.* **108**, 101801 (2012), arXiv:1112.2978 [hep-ex].
- [10] T. Aaltonen *et al.* (CDF Collaboration), *Phys. Rev. D* **89**, 112001 (2014).
- [11] V. M. Abazov *et al.* (D0), *Phys. Rev. Lett.* **100**, 131801 (2008), arXiv:0712.0599 [hep-ex].
- [12] V. M. Abazov *et al.* (D0), *Phys. Rev.* **D88**, 032008 (2013), arXiv:1304.5422 [hep-ex].
- [13] G. Aad *et al.* (ATLAS), *Phys. Rev. Lett.* **116**, 101801 (2016), arXiv:1512.05314 [hep-ex].
- [14] M. Aaboud, G. Aad, *et al.* (ATLAS Collaboration), *Phys. Rev. D* **97**, 032005 (2018).
- [15] M. Aaboud *et al.* (ATLAS), *Phys. Rev.* **D97**, 032005 (2018), arXiv:1709.07703 [hep-ex].
- [16] A. M. Sirunyan, A. Tumasyan, W. Adam, F. Ambroggi, E. Asilar, T. Bergauer, J. Brandstetter, E. Brondolin, M. Dragicevic, and *et al.*, *The European Physical Journal C* **78** (2018), 10.1140/epjc/s10052-018-5567-9.
- [17] A. Senol, *International Journal of Modern Physics A* **29**, 1450148 (2014).
- [18] M. L. Mangano, *The Standard Theory of Particle Physics*, 231 (2016).
- [19] C. Frye, M. Freytsis, J. Scholtz, and M. J. Strassler, *Journal of High Energy Physics* **2016** (2016), 10.1007/jhep03(2016)171.
- [20] T. Dorigo, *Progress in Particle and Nuclear Physics* **100**, 211 (2018).
- [21] A. Senol, H. Denizli, A. Yilmaz, I. T. Cakir, K. Oyulmaz, O. Karadeniz, and O. Cakir, *Nuclear Physics B* **935**, 365 (2018).
- [22] C. Degrande, *Journal of High Energy Physics* **2014** (2014), 10.1007/jhep02(2014)101.
- [23] T. A. Collaboration (The ATLAS Collaboration), *ATLAS-CONF* **2018**, 035 (2018).
- [24] "https://fcc.web.cern.ch/pages/default.aspx," .
- [25] M. Benedikt, M. Capeans Garrido, F. Cerutti, B. Goddard, J. Gutleber, J. M. Jimenez, M. Mangano, V. Mertens, J. A. Osborne, T. Otto, J. Poole, W. Riegler, D. Schulte, L. J. Tavian, D. Tommasini, and F. Zimmermann, "Future Circular Collider," Tech. Rep. CERN-ACC-2018-0058 (CERN, Geneva, 2018) submitted for publication to *Eur. Phys. J. ST*.
- [26] J. Alwall, R. Frederix, S. Frixione, V. Hirschi, F. Maltoni, O. Mattelaer, H.-S. Shao, T. Stelzer, P. Torrielli, and M. Zaro, *Journal of High Energy Physics* **2014** (2014), 10.1007/jhep07(2014)079.
- [27] T. Sjöstrand, S. Ask, J. R. Christiansen, R. Corke, N. Desai, P. Ilten, S. Mrenna, S. Prestel, C. O. Rasmussen, and P. Z. Skands, *Computer Physics Communications* **191**, 159 (2015).

- [28] A. Buckley, J. Ferrando, S. Lloyd, K. Nordström, B. Page, M. Rüfenacht, M. Schönherr, and G. Watt, *The European Physical Journal C* **75** (2015), 10.1140/epjc/s10052-015-3318-8.
- [29] R. D. Ball, V. Bertone, S. Carrazza, C. S. Deans, L. D. Debbio, S. Forte, A. Guffanti, N. P. Hartland, J. I. Latorre, J. Rojo, and M. Ubiali, *Nuclear Physics B* **867**, 244 (2013).
- [30] J. de Favereau, C. Delaere, P. Demin, A. Giammanco, V. Lemaitre, A. Mertens, and M. Selvaggi, *Journal of High Energy Physics* **2014** (2014), 10.1007/jhep02(2014)057.
- [31] P. Demin, "<https://cp3.irmp.ucl.ac.be/projects/exrootanalysis>," .
- [32] R. Brun and F. Rademakers, *Nuclear Instruments and Methods in Physics Research Section A: Accelerators, Spectrometers, Detectors and Associated Equipment* **389**, 81 (1997), new Computing Techniques in Physics Research V.
- [33] V. Khachatryan, A. Sirunyan, A. Tumasyan, W. Adam, E. Asilar, T. Bergauer, J. Brandstetter, E. Brondolin, M. Dragicevic, J. Erö, and et al., *Journal of Instrumentation* **12**, P01020 (2017).
- [34] M. Tanabashi *et al.* (Particle Data Group), *Phys. Rev. D* **98**, 030001 (2018).